

The Therapeutic Effect of Activated Platelet Supernatant-Primed Mobilized Peripheral Blood Mononuclear Cells on Experimentally Induced Ulcers in the Ileum of Adult Male Albino Rat: Histological and Immunohistochemical Study

Original
Article

Aya Abd El-Moneim Abo-Elyazed¹, Amira Adly Kassab^{1,2}, Nadia Abdel Mohsen ElBakry¹, Azza Awad AboRaya¹ and Nawar Mahmoud Shalaby¹

¹Department of Histology and Cell Biology, Faculty of Medicine, Tanta University, Egypt

²Department of Basic Medical Sciences, Faculty of Medicine, Ibn Sina University for Medical sciences, Jordan

ABSTRACT

Introduction: Small-bowel ulcers have many causes and nonsteroidal anti-inflammatory drugs (NSAIDs) represent the most common causes of drug-induced intestinal injury. Peripheral blood mononuclear cell (PBMC) therapy plays an important role in tissue healing and repair, and their priming with activated platelet supernatant (APS) has been known to augment their efficacy through induction of angiogenesis and tissue regeneration.

Aim of the Work: The research aimed to study the influence of APS-primed mononuclear cells on the ileal ulcers induced by indomethacin in adult male albino rats.

Materials and Methods: 45 adult male albino rats were used, 10 of them were used as donors and the other 35 were used as recipient rats which were divided into; group I (acted as a control) and group II were subdivided into subgroup II-A (animals received a single oral dose of 25 mg/kg indomethacin and were sacrificed 6 hours after ulcer induction), subgroup II-B (animals treated by intravenous injection of APS-primed PBMCs after induction of ileal ulcer and were sacrificed after 2 weeks). Finally, the ileum was obtained and processed for histological and immunohistochemical studies.

Results: Subgroup II-A (ulcer induction) revealed marked histological structural changes as focal damage, atrophy of villi, desquamated cells, shrunken irregular cells, darkly stained nuclei, vacuolated cytoplasm, cellular infiltration and congestion of blood vessels. APS-primed mobilized PBMCs therapy induced significant improvement in the histological structure of the ileum (Subgroup II-B).

Conclusion: APS-primed mononuclear cells exerted a significant ameliorative effect on the ileum after ulcer induction by indomethacin.

Received: 17 August 2022, **Accepted:** 13 October 2022

Key Words: APS, ileum, NSAIDs, PBMCs, ulcer.

Corresponding Author: Aya Abd El-Moneim Abo-Elyazed, MSc, Department of Histology and Cell Biology, Faculty of Medicine, Tanta University, Egypt, **Tel.:** +20 10 2023 4213, **E-mail:** aya.aboelyazed@med.tanta.edu.eg

ISSN: 1110-0559, Vol. 46, No. 4

INTRODUCTION

Small-bowel ulcers are frequently recorded in the medical field. They are commonly caused by Crohn's disease, abdominopelvic radiotherapy for cancer, mycotoxins such as aflatoxins, alcohol intake, cytomegalovirus, tuberculous enteritis, bacterial overgrowth, vasculitis, small intestinal diverticula, ischemic ileitis, or drug induction^[1,2]. Many drugs can induce small-bowel ulcers such as potassium, gold, and chemotherapeutic agents. The most common causes of drug-induced intestinal mucosal injury are nonsteroidal anti-inflammatory drugs (NSAIDs) that may cause ulcers, erosions, or broad strictures predominantly in the jejunum and ileum^[3,4].

Cell-based therapy represents a realistic goal for regenerative medicine and has emerged as the most recent and a promising therapeutic strategy with the potential to

treat various diseases, restore damaged tissues and even cure many life-threatening conditions^[5,6]. Among different types of cells that can be used in cell therapy, mononuclear cells play an important role in tissue healing and repair^[7,8].

Mononuclear cells (MNCs) are all blood cells with a single round nucleus and are mainly comprised of T cells, B cells, natural killer (NK) cells, dendritic cells (DCs), and monocytes. These cells play an important role in the immune system which defends the body against infections and destroys tumor cells and foreign substances^[9]. Mononuclear cells are present in a small number in the peripheral blood and accordingly, a granulocyte colony stimulating factor (G-CSF) can be used for mobilizing MNCs from the bone marrow to the peripheral blood^[10,11].

Several studies aimed to increase the effect of cell therapy by using various sources of progenitors, genetic

manipulation of cells, and priming of the cells with various agents such as G-CSF, activated platelet supernatant (APS), angiopoietin-1 (Ang-1), erythropoietin (EPO), and vascular endothelial growth factor (VEGF)^[12]. In a previous report, priming peripheral blood mononuclear cells (PBMCs) with APS has been proven to augment their efficacy through numerous cytokines and chemokines produced by the activated platelets and promote angiogenesis and tissue regeneration^[13,14].

Until now, a few research works have been conducted to detect the outcome of cell therapy on intestinal ulcers. Accordingly, this research aimed to study the effect of APS-primed PBMCs on the induced ulcers in the ileum of adult male albino rats. As NSAIDs are the most common cause of enteropathy, indomethacin was chosen to induce the ileal ulcers as a model in this work.

MATERIALS AND METHODS

Experimental design

The present work was conducted using 45 adult male albino rats; 10 rats served as donors and the other 35 served as recipients. The weights of animals ranged from 150 to 200 grams. All animals were kept in appropriate clean well ventilated cages under the same environmental conditions and were fed a similar laboratory diet and water as recommended by The National Research Council of the National Academies, (2011)^[15]. They were adapted to their environment not less than one week before beginning of the experiment. The recipient rats were divided into two major groups as follows:

Control group (Group I): was subdivided into three equal subgroups (5 rats for each):

- Subgroup I-A: animals kept without interference and sacrificed after 2 weeks.
- Subgroup I-B: animals received 0.5 ml phosphate buffered saline (PBS) (the vehicle used to suspend the primed mobilized PBMCs) once intravenously via tail vein. Then the animals were sacrificed after 2 weeks.
- Subgroup I-C: animals received 1 ml Tween-80 solution (the vehicle used to dissolve indomethacin) orally via oral gavage feeding tube. Then the animals were sacrificed after 6 hours.

Experimental group (Group II): All rats of experimental group were given indomethacin in a dose of 25 mg/kg dissolved in 1 ml Tween-80 and 9 ml 0.9% NaCl once orally via oral gavage feeding tube after overnight fasting for induction of ulcer. Indomethacin is available in the form of capsules (Kahira Pharmaceuticals & Chemical Industries Company, Cairo, Egypt). Then the animals were divided into 2 subgroups (10 rats for each):

- Subgroup II-A: animals were sacrificed 6 hours after induction of ulcer^[16] for ensuring the occurrence of the ulcer.

- Subgroup II-B: animals injected with APS-primed mobilized PBMCs (1×10^7) suspended in 0.5 ml PBS once intravenously via tail vein 24 hours after induction of ileal ulcer and the animals were sacrificed 2 weeks after the injection^[17].

At the appropriate time, the animals were anesthetized by intraperitoneal injection of sodium pentobarbital at dose of 50 mg/kg^[18] and the ileum was carefully dissected and processed for histological and immunohistochemical examination. The bodies of the sacrificed animals were packed in a special package according to the safety precaution and infection control measures then sent with the hospital biohazards. All experimental procedures were approved by the Research Ethics Committee (REC) of Faculty of Medicine, Tanta University, Egypt.

Methods

This experiment was carried out at the Tissue Culture Unit of the Histology and Cell Biology Department in Faculty of Medicine, Tanta University, Egypt.

Ten rats were used as donor rats (five rats for isolation of PBMCs and five rats for preparation of APS).

Isolation of peripheral blood mononuclear cells

At first, the rats received granulocyte colony-stimulating factor (G-CSF) injection subcutaneously at a dose of 100 µg/kg once daily for 3 consecutive days to mobilize MNCs to the peripheral blood systems^[13]. G-CSF or Filgrastim (Neupogen) is available in the form of a pre-filled syringe / solution (Amgen, USA). At the end of third day, peripheral blood collection was performed by cardiac puncture following sterilization of the thorax using alcohol then the PBMCs were isolated by density gradient centrifugation method^[19].

In general, anticoagulant-treated blood was diluted with a balanced salt solution, carefully layered over the separation medium (Ficoll-Paque product) without intermixing and centrifuged for 30-40 min. During centrifugation, differential migration of cells resulted in formation of layers with different cell types. Accordingly, on top of the separation medium, mononuclear cells and platelets were found because of their low density. On the other hand, red blood cells and granulocytes, which have a higher density, were found at the bottom layer. Platelets were separated from the mononuclear cells by subsequent washing by PBS^[20].

Preparation of activated platelet supernatant

At first, platelet rich plasma (PRP) was separated by centrifugation then it was activated with calcium gluconate. After that, the activated-platelet content was centrifuged, and the supernatant was used for priming^[21].

PRP preparation

Platelet rich plasma was prepared by a differential centrifugation process in which particular cellular components were precipitated according to various

specific gravity^[22]. The first centrifugation was performed to separate red blood cells and followed by another centrifugation for concentration of the platelets, which were present in the smallest final volume of plasma^[23,24].

PRP activation

Activation of PRP was performed by adding 0.1 ml of calcium gluconate (10%) to each 1 ml of PRP samples. Then the activated PRP sample was incubated for 24 hours at 37° C for platelet gel formation. After that, the sample was centrifuged at 2800 ×g for 15 minutes at 20° C, and the supernatant was taken for priming^[25,26].

Finally, following isolation of PBMCs and preparation of APS, the PBMCs was co-cultured with APS in 5% CO₂ incubator at 37°C for 6 hours^[13]. Then, APS-primed mobilized PBMCs (1×10⁷) suspended in 0.5 ml PBS were injected once intravenously via tail vein 24 hours after induction of ileal ulcer and the animals were sacrificed 2 weeks after the injection^[17].

Histological and immunohistochemical studies

I – Histological studies

A piece of ileum of each sample was immediately immersed in buffered formalin solution then processed for preparation of paraffin block, 5 µm thick sections were obtained using rotary microtome and were stained with Haematoxylin and eosin (H&E) stains and Combined (Periodic acid Schiff - Alcian blue) (PAS-AB) stain and examined by light microscope^[27].

Another small pieces of ileum were placed in 2.5% buffered glutaraldehyde solution for fixation and then processed by routine protocol of transmission electron microscope. Semithin sections of 1 µm thickness were obtained, stained with toluidine blue and examined to select good fields for photography. Ultrathin sections of 40-150 nm thickness were stained using lead citrate and uranyl acetate for examination then photographed using (JEOL-JEM-100 SX EM, Japan) at the Electron Microscopy Unit in the Faculty of Medicine, Tanta University^[28].

II- Immunohistochemical studies

Ileal sections were stained for detection of proliferating cell nuclear antigen (PCNA)^[29,30] as follow: sections were deparaffinized by immersion in xylene series, rehydrated through descending grades of ethanol, placed into PBS, and heated in a microwave oven (700 W for 5 min) to unmask the antigen. After that, sections were left for 20 min in 3% hydrogen peroxide solution to inhibit formation of background staining resulting from endogenous peroxidase activity. Non-specific binding sites were blocked by incubation of the sections in blocking solutions. The sections were incubated with mouse anti-PCNA monoclonal antibody (clone pc 10) (from Labvision Inc., Fremont, CA, USA, dilution of 1:100) staying the night in a humid room at 4 °C and followed by incubation with biotinylated rabbit anti-mouse Ig (1:200 dilution) for 60 minutes at room temperature. Next, they were

subjected to horseradish peroxidase-streptavidin (ScyTek UHP 125, USA) at room temperature for 20 min. The immunoreactivity was visualized using freshly prepared diaminobenzidine (DAB) as a chromogen and sections were counterstained with Mayer's haematoxylin. Finally, sections were dehydrated in ascending grades of alcohol then cleared in xylene, mounted in Canada balsam, and examined under light microscope. For obtaining negative control, the same procedure was performed, but the primary antibody was excluded. The cellular site of the reaction was nuclear and attained brown coloration.

Lastly, examination and photographing of sections were performed using (Leica compound light microscope with built in camera) at the Histology and Cell Biology Department and (Olympus light microscope, BX43) at Microbiology Department, Faculty of Medicine, Tanta University.

Morphometric Study

The mean number of the following cells were analyzed:

1. Goblet cells stained with (PAS-AB) stain was carried out in villi and crypts with a magnification power of (×200).
2. Positive nuclei for PCNA was performed in the crypts with a magnification power of (×400).

10 randomly chosen microscopic fields in each specimen were examined by Image J software program (National Institute of Health, Bethesda, Maryland, USA).

Statistical analysis

Analysis of data was conducted by one-way analysis of variance (ANOVA) and comparison between the groups was done by Tukey's test utilizing statistical package for Graph Pad Instate software (version 3, USA). After that, expression of all values as means ± standard deviation was performed. If the *P-value* <0.05, the differences were significant and if *P value* > 0.05 the differences were considered nonsignificant^[31].

RESULTS

Light microscopic results

H&E-stained section

Examination of sections of the control subgroups (subgroup I-A, I-B &I-C) revealed the same histological picture of the ileum. The wall of ileum was composed of mucosa, submucosa, muscularis and serosa (Figure 1). The ileal mucosa was formed of epithelium, lamina propria and muscularis mucosa. The mucosa showed finger-like projections (villi) with a core of connective tissue containing blood vessels. The epithelium lining the villi was composed of enterocytes having regular continuous brush border, acidophilic cytoplasm and oval basal vesicular nuclei. The goblet cells exhibited frequent clear empty spaces among the enterocytes (Figure 2). Also, the mucosa showed tubular glands (crypts of Libierkühn)

which appeared as invaginations into the lamina propria. The epithelium lining crypts was composed of enterocytes, goblet cells and Paneth cells that appeared at the base of the crypts and characterized by eosinophilic granules (Figure 3).

Examination of sections obtained from subgroup II-A (6 hours after induction of ileal ulcer) revealed marked histological structural changes in the form of disrupted villi and crypts architecture. The mucosa appeared with focal loss of villi, sloughing of epithelial cells covering the remaining villi and alteration of the shape of the crypts (Figures 4,5). Other villi appeared broad with subepithelial space and shrunken irregular cells. Cellular infiltration and congestion of blood vessels in the lamina propria were also observed (Figures 5,6).

As regards subgroup II-B (animals injected with APS-primed mobilized PBMCs suspended in PBS 24 hours after induction of ileal ulcer and sacrificed after 2 weeks), it showed significant improvement of ileal mucosal architecture as compared to subgroup II-A. Most of the villi appeared intact having a core of lamina propria with enterocytes and goblet cells near that of the control group (Figures 7,8). Also, the crypts showed enterocytes, goblet cells and Paneth cells near that of the control group. Few enterocytes lining the crypts still appeared with cytoplasmic vacuoles (Figure 9).

Combined Periodic acid Schiff - alcian blue (PAS-AB) stain

Sections obtained from the control subgroups showed strong PAS-AB positive reaction (blue color) in the goblet cells over the villi and crypts. The brush border of enterocytes appeared with strong PAS positive reaction (magenta color) (Figure 10). Sections obtained from subgroup II-A showed focal areas with apparently few goblet cells over the villi and crypts exhibiting PAS-AB positive reaction (due to sloughed enterocytes and goblet cells). Complete depletion of mucous with PAS-AB negative reaction was also detected in some goblet cells. Lost brush border of most enterocytes was also observed (Figure 11). On the other hand, sections obtained from subgroup II-B showed numerous goblet cells distended with mucous with an apparent strong PAS-AB positive reaction. Well-defined brush border of the enterocytes with strong PAS positive reaction was also observed (Figure 12).

Immunohistochemical results for proliferating cell nuclear antigen (PCNA)

Examination of sections obtained from control subgroups revealed a strong PCNA positive reaction in the nuclei of many enterocytes in the crypts (Figure 13). Sections obtained from subgroup (II-A) revealed a weak positive reaction for PCNA in the nuclei of some cells and negative reaction in the nuclei of many cells in the crypts (Figure 14). On the contrary, sections obtained from subgroup (II-B) revealed a strong PCNA positive reaction

in the nuclei of numerous cells in the crypt region when compared to subgroup II-A (Figure 15).

Results for statistical analysis

The mean number of goblet cells (Table 1, Bar Chart 1): The Tukey-Kramer test detected no significant difference in the mean number of goblet cells of control subgroups (I-A, I-B& I-C) when compared with each other. Subgroup (II-A) revealed a significant reduction when compared with control group, while subgroup II-B showed significant increase in comparison with subgroup (II-A). Moreover, this test revealed no significant difference between subgroup (II-B) and control group.

Statistical Results for the mean number of PCNA positive nuclei (Table 2, Bar Chart 2): The Tukey-Kramer test revealed no significant difference in the mean number of PCNA positive nuclei between the control subgroups. Subgroup (II-A) revealed a significant reduction in the mean number of PCNA positive nuclei in comparison with control group, while subgroup II-B showed significant increase in comparison with subgroup (II-A).

Electron microscopic results

Ultrathin sections obtained from rat ileum of the control group revealed absorptive cells (enterocytes) with regularly arranged closely packed apical microvilli, rounded to oval basal nuclei in addition to presence of abundant elongated mitochondria. Theliolymphocytes (intraepithelial lymphocytes) were detected with large nucleus and peripherally arranged chromatin, clear cytoplasm, and abundant ribosomes (Figure 16). Goblet cells were insinuated between the enterocytes with distended apical part containing moderately electron dense mucin-secretory granules and compressed basal part containing nucleus and RER (Figure 17). Additionally, Paneth cells appeared with short microvilli, basal nuclei and apical membrane-bound secretory granules having electron dense core surrounded by a light halo (Figure 18).

Sections obtained from subgroup II-A revealed destroyed luminal surface of the enterocytes with corrugation of the nuclear membrane and dilated perinuclear space. Moreover, the cytoplasm showed swollen mitochondria with lost cristae, dilated RER and massive cytoplasmic rarefaction (Figures 19,20). As regards the goblet cells, they showed an apparent decrease in their secretory granules. Some granules appeared irregular in shape and others fused together with depletion of their secretion. Also, their cytoplasm revealed dilated RER and cytoplasmic rarefaction (Figure 21). In addition, Paneth cells showed shrunken nuclei with condensed chromatin and destroyed cristae of mitochondria. Some cells showed abnormal granules with feathery edges (Figure 22). In the lamina propria, cellular infiltration of eosinophils, mast cells and lymphocytes as well as congested blood vessels were observed (Figure 23).

Examination of sections obtained from subgroup II-B revealed significant improvement as compared to

subgroup II-A. Enterocytes appeared with preserved regularly arranged microvilli, intact lateral interdigitations and rounded to oval nuclei besides apparently normal elongated mitochondria (Figure 24). Additionally, goblet cells near that of the control group were noticed among enterocytes having apical part distended with mucin granules and basal part containing compressed nucleus and RER (Figure 25). As regards Paneth cells, they appeared with apical cytoplasmic membrane bound electron dense homogenous secretory granules. Some cells appeared with irregular nuclear membrane outline (Figure 26).

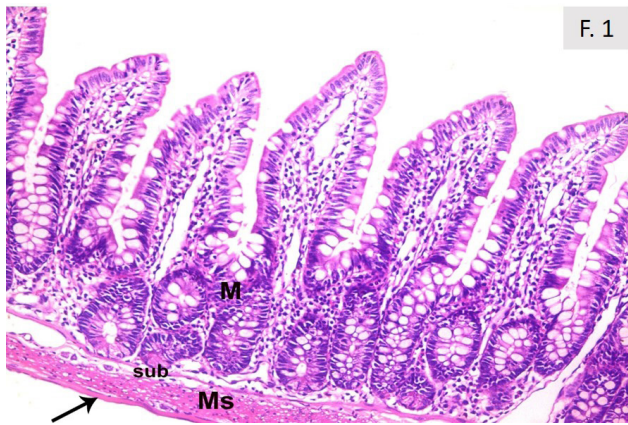


Fig. 1: shows mucosa (M), submucosa (Sub), muscularis (Ms) and serosa (→). (H& E, control × 200)

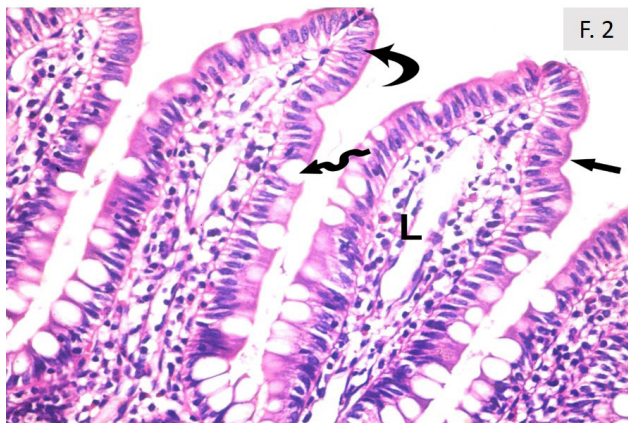


Fig. 2: shows the intestinal villi (→) with a core of lamina propria (L). The villi are covered with simple columnar absorptive cells with basal oval nuclei, acidophilic cytoplasm and regular continuous brush border (Curved arrow). Notice the presence of goblet cells in between the columnar cells (Wavy arrow). (H& E, control × 400)

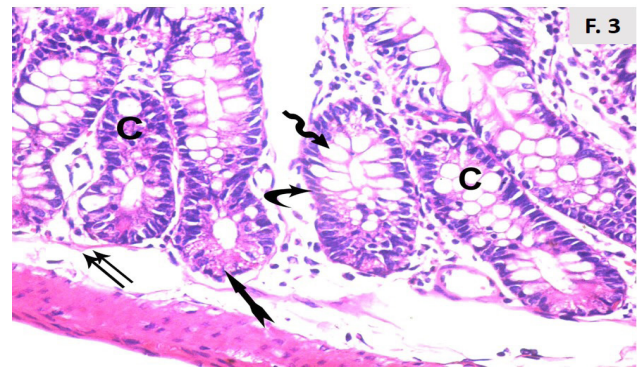


Fig. 3: shows tubular crypts of Lieberkühn (C). The crypts are lined with columnar absorbing cells (curved arrow) and goblet cells (wavy arrow). Paneth cells can be seen at the base of the crypts (bifid arrow). Notice the presence of muscularis mucosa (double arrow) in between mucosa and submucosa. (H& E, control × 400)

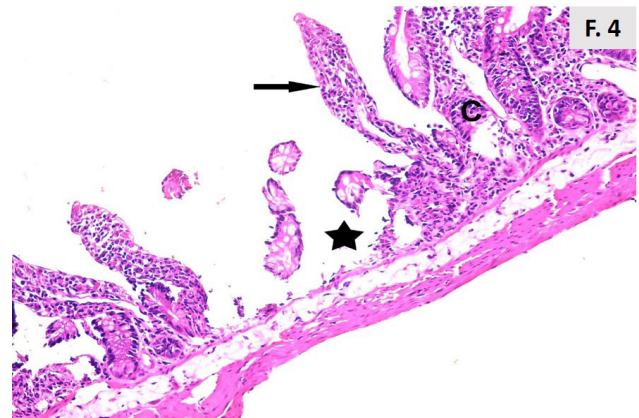


Fig. 4: shows focal loss of villi (*), sloughing of epithelial cells covering the remaining villi (→), and alteration of the shape of the crypts (C). (H& E, subgroup II-A, × 200)

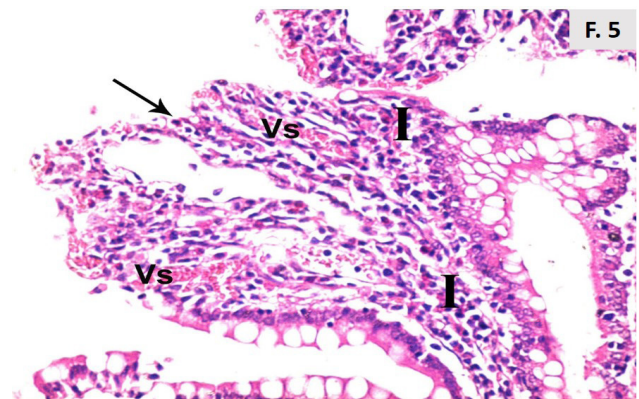


Fig. 5: shows cellular infiltration (I) and congested blood vessels (Vs) in the core of the villi as well as sloughing of surface epithelial cells (→). (H& E, subgroup II-A, × 400)

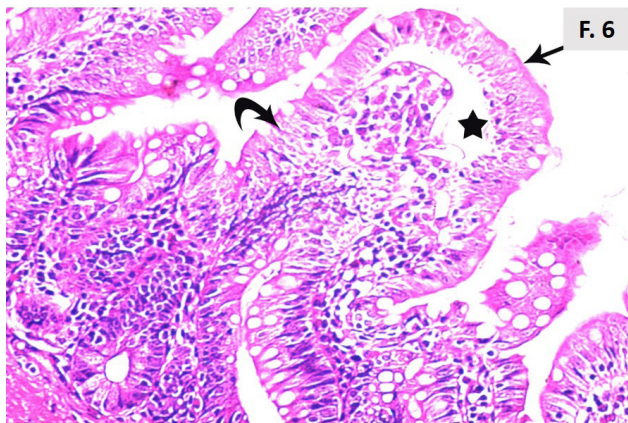


Fig. 6: shows broad villi (→) with subepithelial space (*) and shrunken irregular cells (curved arrow). (H& E, subgroup II-A, × 400)

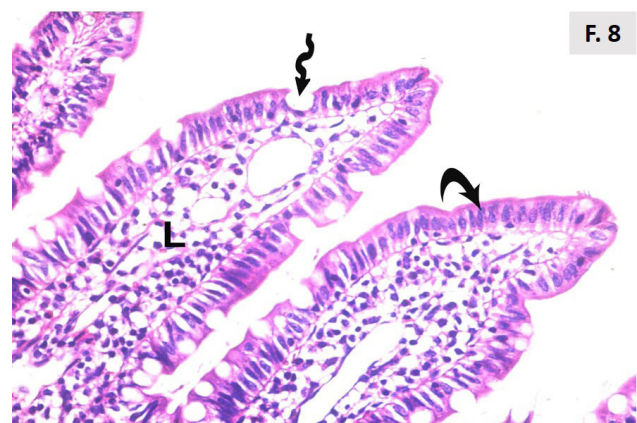


Fig. 8: shows intact villi with a core of lamina propria (L). The villi are covered with nearly normal enterocytes (curved arrow) and goblet cells (wavy arrow). (H& E, subgroup II-B, × 400)

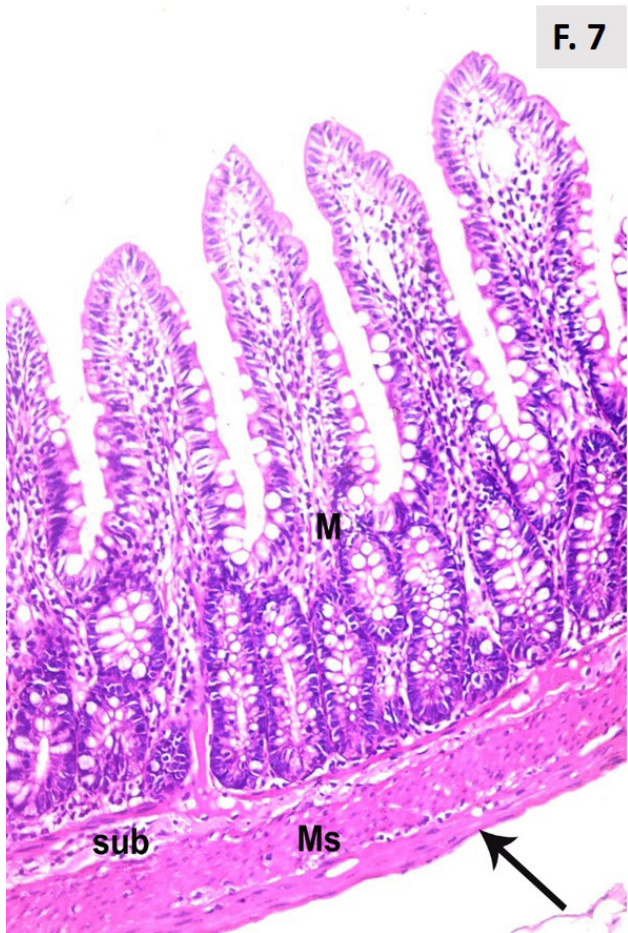


Fig. 7: shows nearly normal ileal mucosal architecture (M) with intact villi and crypts. Notice submucosa (Sub), muscularis (Ms) and serosa (→) appear normal. (H& E, subgroup II-B, × 200)

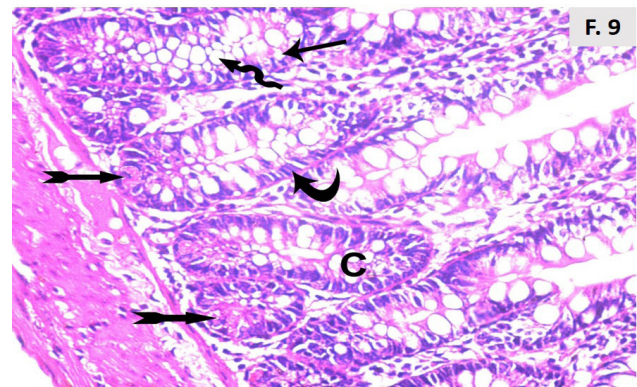


Fig. 9: shows nearly normal crypt architecture (C) lined with enterocytes (curved arrow), goblet cells (wavy arrow) and Paneth cells (bifid arrow) at the base of the crypts. A few enterocytes appear with cytoplasmic vacuoles (→). (H& E, subgroup II-B, × 400)

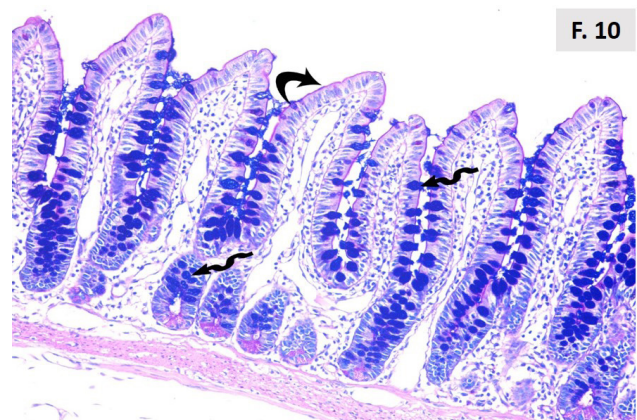


Fig. 10: shows strong PAS-AB positive reaction in the goblet cells (wavy arrow) of villi and crypts. Strong PAS positive reaction in the brush border of enterocytes is observed (curved arrow). (PAS-AB, control, × 200)

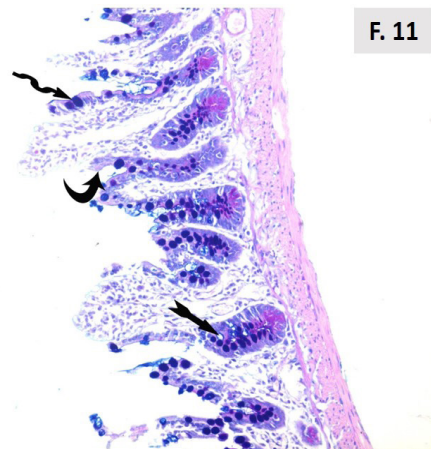


Fig. 11: shows apparently few goblet cells (wavy arrow) with positive reaction over the villi and crypts. Some goblet cells appear completely depleted of mucous and are PAS-AB negative (bifid arrow). Notice lost brush border of most enterocytes (curved arrow). (PAS-AB, subgroup II-A, $\times 200$)

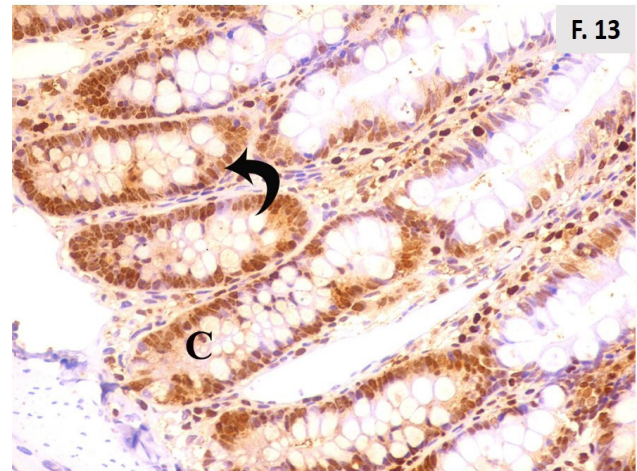


Fig. 13: shows strong PCNA positive reaction in the nuclei (curved arrow) of many enterocytes in the crypt region (C). (PCNA, control $\times 400$)

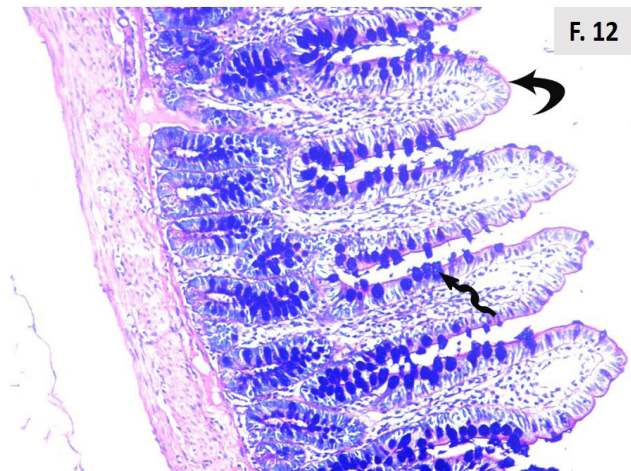


Fig. 12: shows numerous goblet cells distended with mucous with an apparent strong PAS-AB positive reaction (wavy arrow). Well-defined brush border of enterocytes appears with strong PAS positive reaction (curved arrow). (PAS-AB, subgroup II-B, $\times 200$)

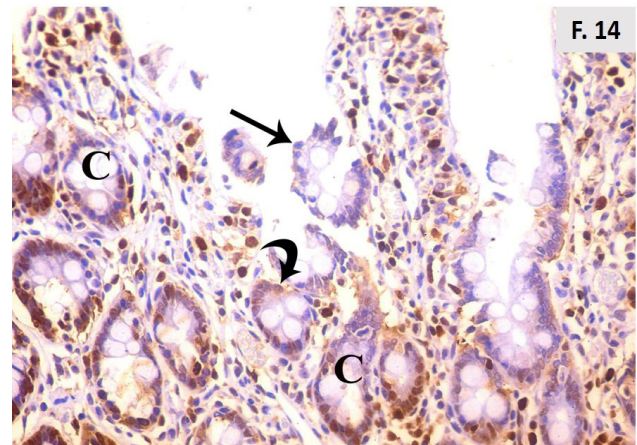


Fig. 14: shows a weak PCNA positive reaction in the nuclei (curved arrow) of some cells and negative reaction in the nuclei (\rightarrow) of many enterocytes in the crypt region (C). (PCNA, subgroup II-A $\times 400$)

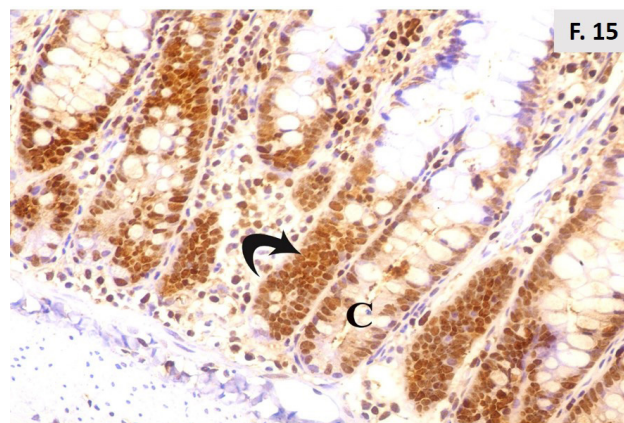


Fig. 15: shows a strong positive reaction in the nuclei of numerous enterocytes (curved arrow) in the crypt region (C) when compared to subgroup II-A. (PCNA, subgroup II-B $\times 400$)

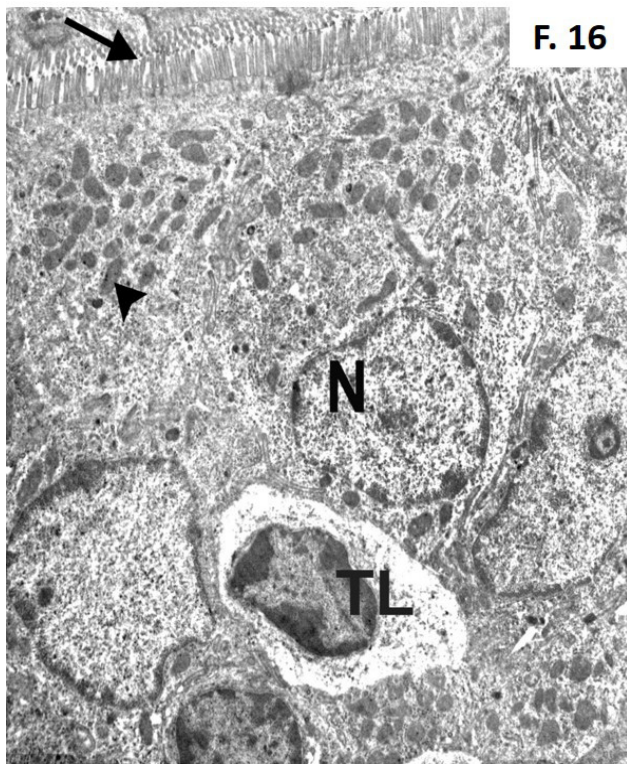


Fig. 16: shows enterocytes with regularly arranged closely packed apical microvilli (→), rounded to oval basal nuclei (N) and apical mitochondria (▴). Notice: Thelio-lymphocyte (intraepithelial lymphocyte) (TL) in between enterocytes. (control, × 1500)

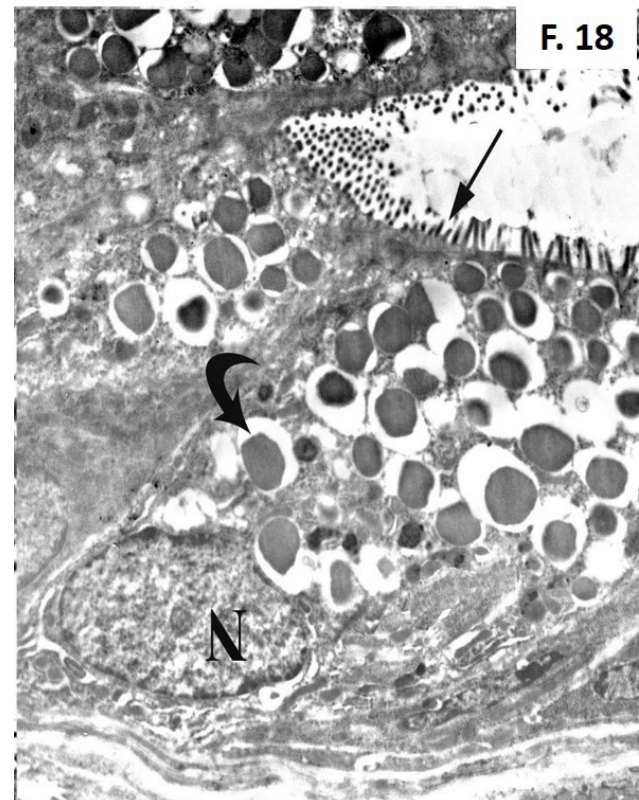


Fig. 18: shows Paneth cells with short microvilli (→), basal euchromatic nuclei (N) and apical large membrane-bound secretory granules with a dense core surrounded by a light halo (curved). (control, × 1500)

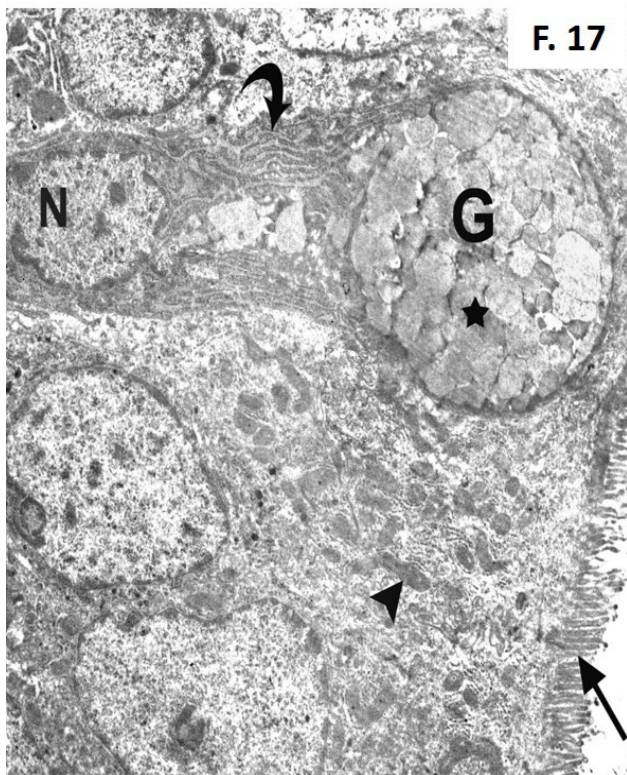


Fig. 17: shows a goblet cell (G) in between enterocytes with distended apical part containing mucin-secretory granules (*) and compressed basal part containing nucleus (N) and RER (curved). Notice enterocytes with apical regularly arranged microvilli (→) and mitochondria with dense cristae (▴). (control, × 1500)

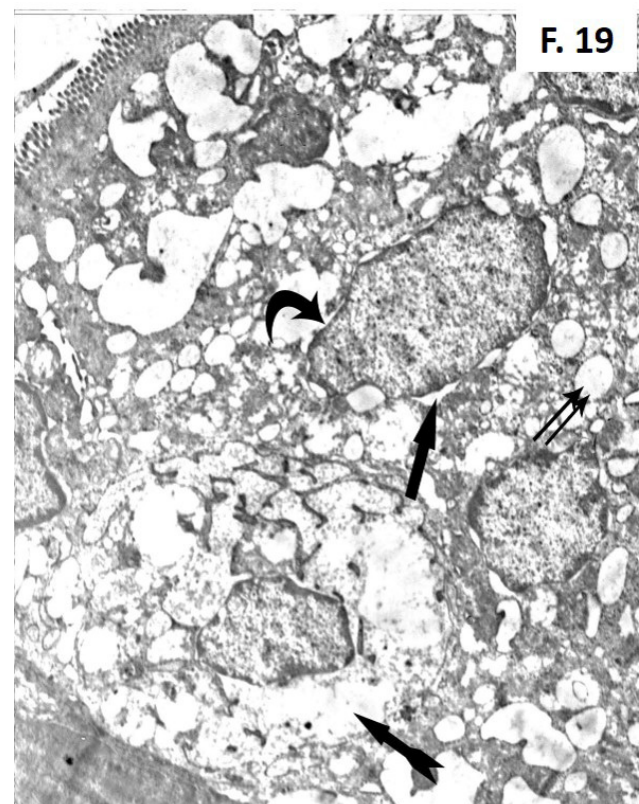


Fig. 19: shows enterocytes with corrugation of the nuclear membrane (curved), dilated perinuclear space (→), dilated RER (double arrow) and massive cytoplasmic rarefaction (bifid arrow). (subgroup II-A, × 1500)

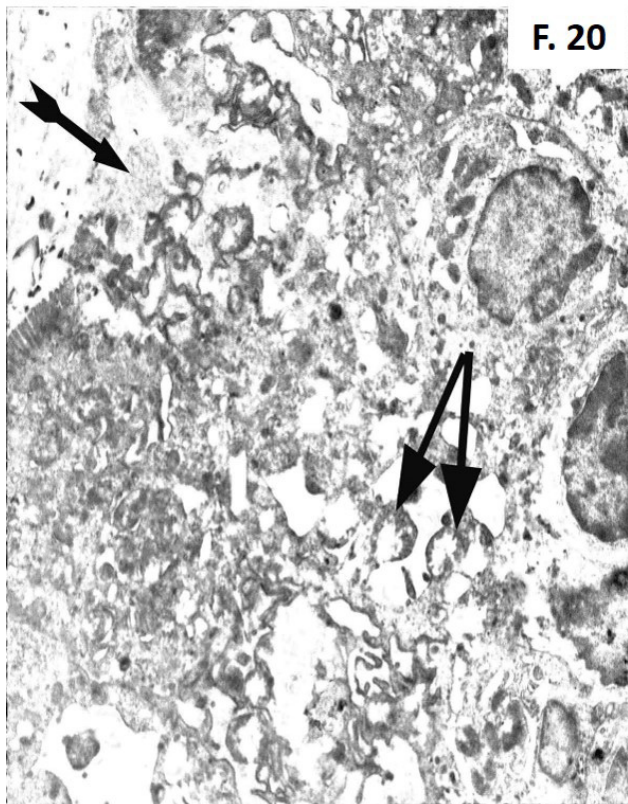


Fig. 20: shows enterocytes with destroyed luminal surface (bifid arrow) and swollen mitochondria with lost cristae (→). (subgroup II-A, × 1500)

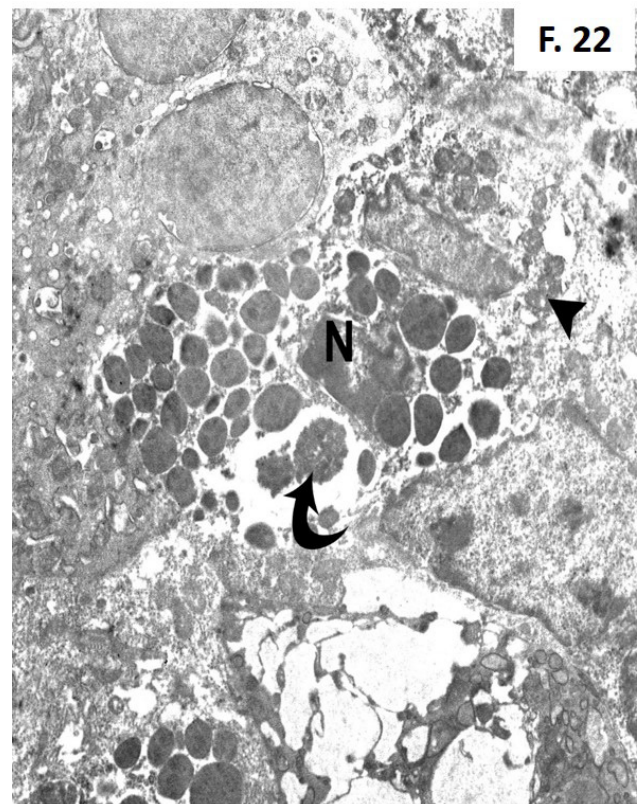


Fig. 22: shows Paneth cells with shrunken nucleus exhibiting condensed chromatin (N), destroyed cristae of mitochondria (▶) and abnormal granules with feathery edges (curved arrow). (subgroup II-A, × 1500)

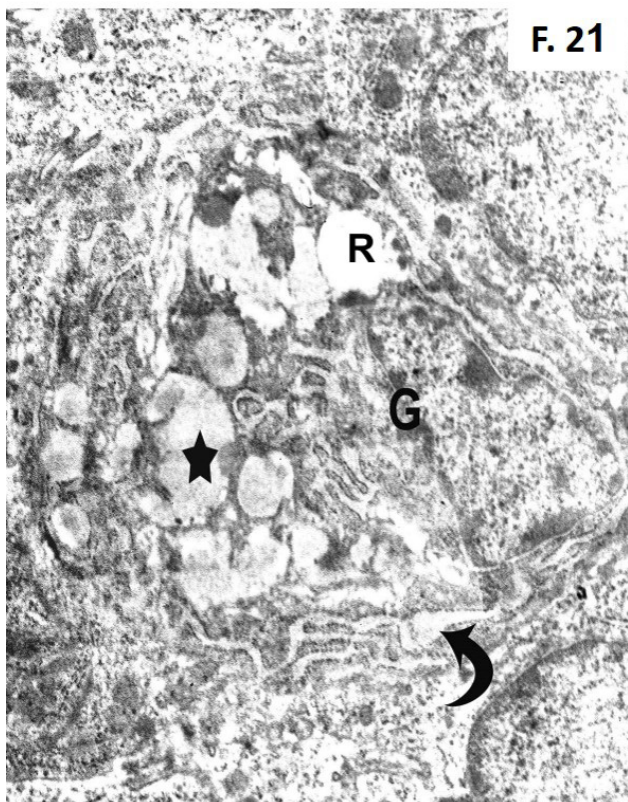


Fig. 21: shows a goblet cell (G) with apparent decrease of secretory granules with irregular shape. Some secretory granules are fused with each other with depletion of their secretion (*). Dilated RER (curved arrow) and cytoplasmic rarefaction (R) are seen. (subgroup II-A, × 3000)

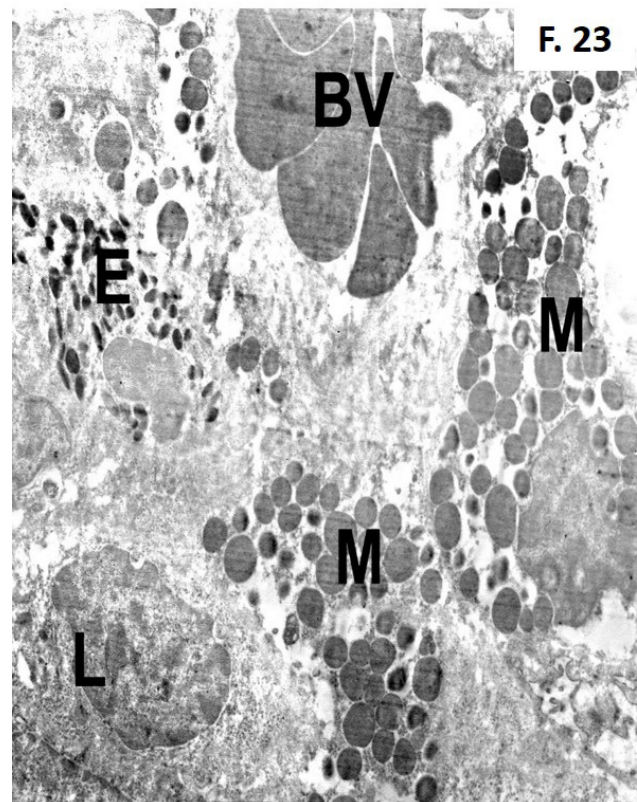


Fig. 23: shows cellular infiltration with a lymphocyte (L), an eosinophil (E) and mast cells (M). Notice congested blood capillary (BV) in the lamina propria. (subgroup II-A, × 1500)

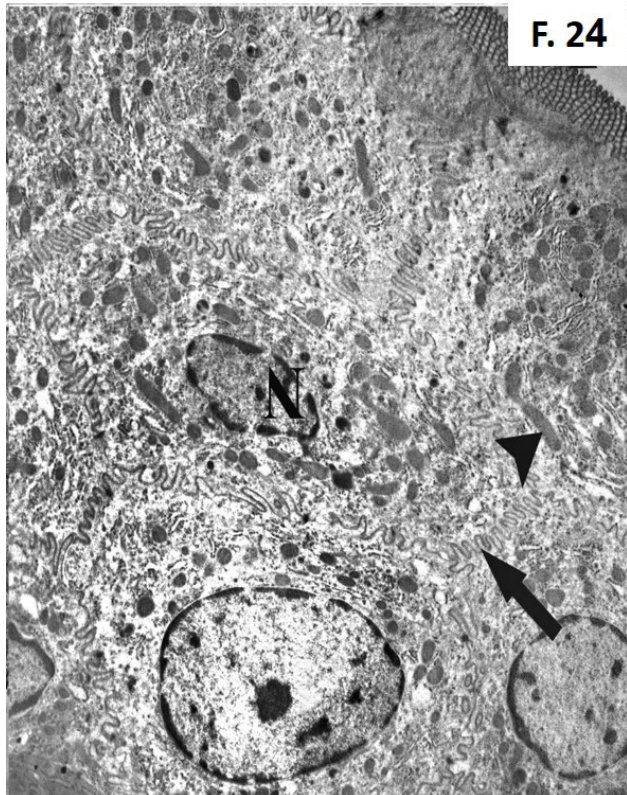


Fig. 24: shows enterocytes with regularly arranged microvilli (→), intact lateral interdigitations (thick arrow), and apparently normal elongated mitochondria (▶). Notice an enterocyte with small nucleus and irregular nuclear membrane (N) (subgroup II-B, × 1500)

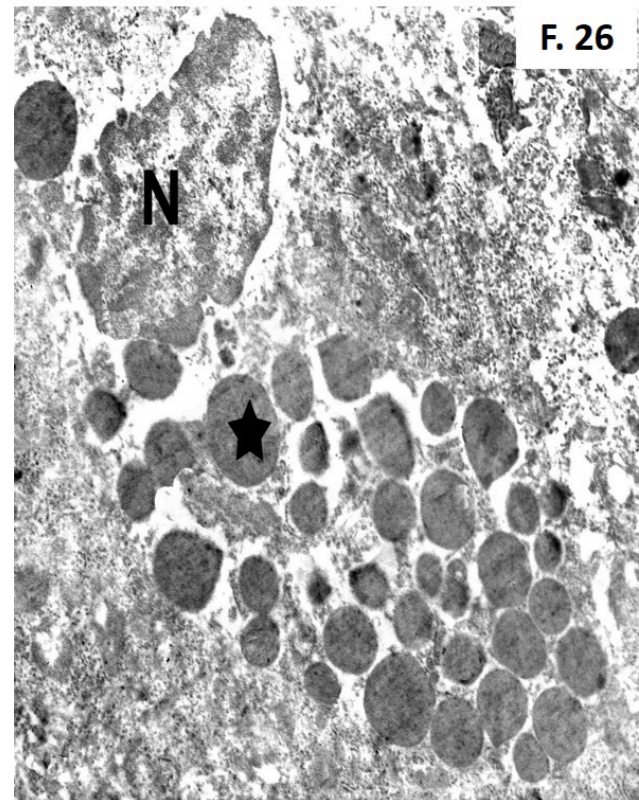


Fig. 26: shows Paneth cell with basal nucleus (N) exhibiting irregular nuclear membrane and apical membrane bound electron dense homogenous secretory granules (*). (subgroup II-B, × 2500)

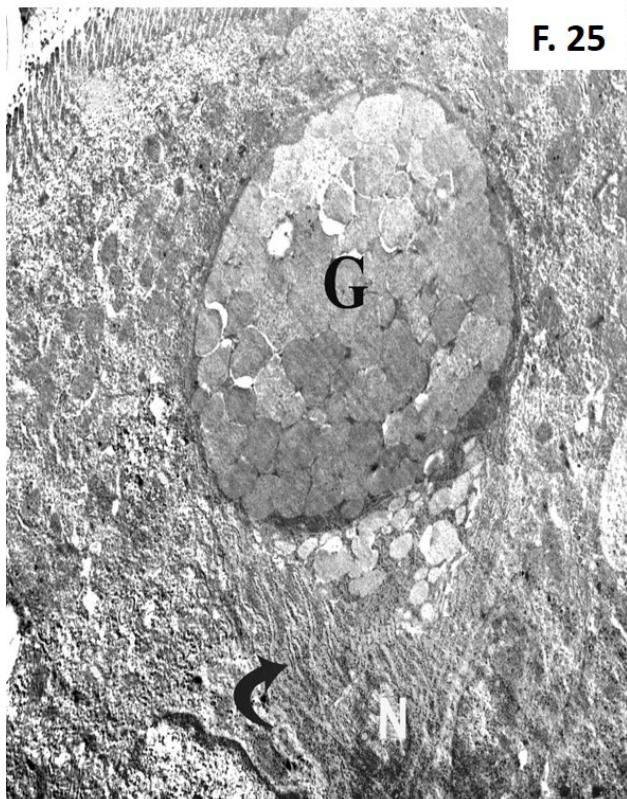


Fig. 25: shows a goblet cell (G) in between enterocytes with apical part distended with mucin granules and basal part containing compressed nucleus (N) and RER (curved arrow). (subgroup II-B, × 1500)

Table 1: Mean number of goblet cells

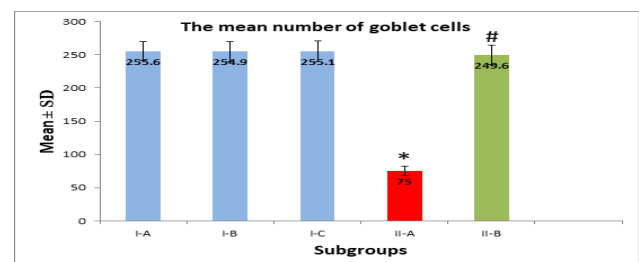
	Control group (G-I)			Experimental group (G-II)	
	Subgroup (I-A)	Subgroup (I-B)	Subgroup (I-C)	Subgroup (II-A)	Subgroup (II-B)
Mean	255.6	254.9	255.1	75*	249.6*
SD	13.9777	14.8582	16.0516	7.1802	14.7888

* significant relative to control; # significant relative to subgroup II-A.

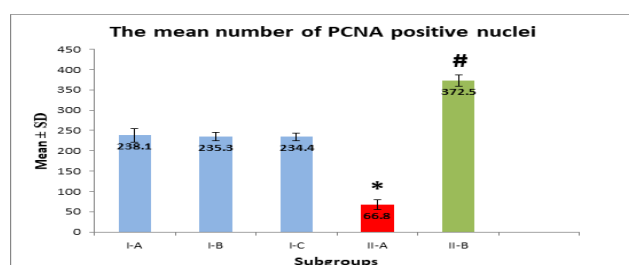
Table 2: Mean number of PCNA positive nuclei

	Control group (G-I)			Experimental group (G-II)	
	Subgroup (I-A)	Subgroup (I-B)	Subgroup (I-C)	Subgroup (II-A)	Subgroup (II-B)
Mean	238.1	235.3	234.4	66.8*	372.5*
SD	17.2204	10.8735	9.0209	11.9238	14.2458

* significant relative to control; # significant relative to subgroup II-A.



Bar chart 1: Mean number of goblet cells



Bar chart 2: Number of PCNA positive nuclei

DISCUSSION

This research was designed to study the influence of APS-primed PBMCs on the induced ulcers in the ileum of adult male albino rats. As NSAIDs are common cause of enteropathy, indomethacin was used to induce ileal ulcer^[16].

Examination of sections obtained from subgroup II-A represented marked histological structural changes revealing disrupted villi and crypts architecture. The mucosa appeared with atrophy and focal loss of villi. Some villi showed sloughing of surface epithelial cells, while others appeared broad with subepithelial spaces. Congestion of blood vessels together with cellular infiltration were also detected in the lamina propria. These results agreed with other studies of small intestinal ulcers in rat^[16,32].

Ishii *et al.* (2019) and Cervantes-García *et al.* (2020)^[33,34] attributed NSAIDs-induced intestinal mucosal damage to inhibition of cyclooxygenase-1 (COX-1) enzyme and reduction of prostaglandin E2 (PGE2) synthesis with vasoconstriction and decrease in the blood flow of mucosa in addition to reduction in bicarbonate and mucus production with subsequent loss of mucosal defense and repair. They added that inhibition of PGE2 synthesis might adhere large number of neutrophils to the vascular endothelium resulting in microvascular stasis, ischemia and release of oxygen derived free radicals leading to mucosal injury. Furthermore, NSAIDs as weak lipophilic acids promote regional irritant effect because they interact with phospholipids of the brush border with direct damage to the surface epithelium^[35].

Moreover, the villus and crypt damage seen in the present work, could be also attributed to the generation of oxygen free radicals and reactive oxygen species (ROS) that occurs due to mitochondrial dysfunction, infiltration of neutrophils into the mucosa, and activation of xanthine oxidase enzyme or a combination of these factors^[36-38]. They added that excessive production of these free radicals leads in oxidative stress during which the free radicals can react with and induce damage to DNA, lipids, and proteins. Additionally, the excessive formation of ROS could induce endothelial barrier dysfunction with subsequent increase in permeability to fluids and solutes causing mucosal edema in the connective tissue stroma as well as beneath the villus absorbing cells resulting in detachment of the lamina propria from the surface epithelium and appearance of subepithelial spaces^[39,40].

The PAS-AB staining results of subgroup II-A showed an apparent reduction in the number of goblet cells and confirmed by EM which revealed an apparent reduction in number of their secretory granules with depletion of secretion. These findings might be due to a decrease of the MUC2 protein levels by NSAIDs with subsequent reduction in stored mucin in goblet cells and a deficient mucus barrier^[41,42]. Furthermore, there was a significant reduction in the mean number of PCNA positive nuclei when compared with control group. This could be attributed to inhibition of DNA synthesis and reduction of mitosis in the cells of crypts due to ulcer damage^[43].

Electron microscopic examination revealed shrunken nuclei with condensed chromatin. This could be attributed to mitochondrial dysfunctions causing changes in the mitochondrial membrane permeability and release of cytochrome c as well as activation of the caspase cascade, resulting in apoptotic cell death with subsequent DNA fragmentation and chromatin condensation^[44]. Additionally, corrugation of the epithelial cells nuclear membranes and dilated perinuclear space could be due to lipid peroxidation of polyunsaturated fatty acids of the biological membranes and protease enzyme activation leading to disintegrating the intermediate filaments forming the nuclear lamins with nuclear membrane affection^[45,46].

In the present study, swelling of mitochondria with destroyed cristae could be considered as an initial event occurring after cell damage where vacuoles exist within the mitochondria deforming the normal regular cristae^[47]. This might be due to inhibition of electron transport and uncoupling of oxidative phosphorylation leading to decreased cellular ATP production and cellular calcium toxicity which activate several enzymes with potentially injurious cellular effects^[46,48]. Additionally, these enzymes lead to destruction of the proteins of membranes and cytoskeletal elements resulting in shortening in addition to focal loss of microvilli and lost brush border of most enterocytes^[49].

Dilatation of RER was observed and could be attributed to accumulation of secretory products as well as disturbance in protein synthesis in response to cell injuries^[50]. In addition, rarefaction of the cytoplasm observed in our study could be due to cellular swelling that associated with increasing cellular membranes permeability. This was explained by diluted cytoplasm as a result of increasing cell volume without an increase in the cell organelles resulting in appearance of electron lucent areas in the cytoplasm referred as cytoplasmic rarefaction or cytoplasmic edema^[51].

Moreover, Paneth cells showed abnormal granules with feathery edges. This might be due to interruption of macroautophagy in intestinal epithelial cells. In Paneth cells, as autophagy can regulate the excretion of antimicrobial proteins and peptides, therefore, without autophagy, these cells cannot properly secrete their compounds leading to structural abnormalities and abnormal morphology of secretory granules^[52].

Congestion of blood vessels in addition to cellular infiltration were also noticed in the lamina propria. This could be due to release of pro-inflammatory cytokines such as TNF- α and IL-6 which provoke inflammatory response resulting in relaxation of vascular smooth muscle and congestion to bring more blood to the inflamed site^[53-55]. They added that endothelial cell intercellular adhesion molecule-1 (ICAM-1) and mucosal addressin cell adhesion molecule-1 (MAdCAM-1) together with leukocyte $\alpha 4 \beta 1$ & $\alpha 4 \beta 7$ and $\beta 2$ integrins are released during inflammation and act as primary mediators of leukocyte recruitment.

As regards subgroup II-B, it showed significant improvement when compared to subgroup II-A. This was agreed with Kang *et al.* (2016)^[13] who revealed that APS-primed mobilized PBMCs promote angiogenesis, tissue healing and repair as evidenced in models of mouse ischemic limb and myocardial infarction.

Mononuclear cells have antioxidant, anti-inflammatory, and cytoprotective effects due to reduced cell death and increased cell proliferation in addition to presence of multipotent progenitor cell populations such as HSCs, mesenchymal stem cells (MSCs), endothelial progenitor cells (EPCs), as well as a population of circulating fibrocytes, so they have the potential to differentiate into a multitude of mature functional cell types in specific sites^[11,56,57].

Moreover, Kang *et al.* (2016) and Escobar *et al.* (2018)^[13,21] revealed that APS contain increased levels of cytokines (IL-1 β , IL-10, and TGF β) which participate in macrophages (M2) polarization reversing the ratio of M1 (Proinflammatory macrophages) /M2 (reparatory-type macrophages) approximately from 4:1 to 1:2.5. M2 macrophages are characterized by their anti-inflammatory effect and promoting angiogenesis helping in tissue regeneration and remodeling. They added that the primed mononuclear cells can recruit appropriate host cells through a paracrine effect and increasing their adhesion to the endothelial cells and extracellular matrix.

In this subgroup, the PAS-AB staining results exhibited significant increase in the mean number of goblet cells in comparison with subgroup II-A. This might be due to the therapeutic effect that improved the mucosal regeneration and reepithelization^[49]. Furthermore, the mean number of PCNA positive nuclei showed significant increase in comparison with subgroup II-A. This could be due to homing of PBMCs to the injured intestinal areas as a response to chemoattraction factors secreted in the inflamed tissues and its differentiation into epithelial and immune cells^[56,58].

CONCLUSION

APS-primed PBMCs injection could ameliorate the induced ileal ulcer of adult male albino rats.

RECOMMENDATIONS

- It is recommended to use APS-primed mononuclear cells as a novel therapy for small intestinal ulcers.
- Further studies using more rats with different durations of follow up are required to find out the stages and various mechanisms by which APS-primed mononuclear cells can promote ulcer healing.
- More studies are required to detect the effect of priming agents other than APS.

ACKNOWLEDGEMENT

I would like to extend my deep appreciation to all the technicians in Histology and Cell Biology Department and Electron Microscope Unit, Faculty of Medicine, Tanta University, for their help throughout this work.

CONFLICT OF INTERESTS

There are no conflicts of interest.

REFERENCES

1. Amer RM: The Possible Protective Role of Zingerone on Ethanol Induced Entrotoxicity of Jejunum in Adult Albino Rats: Light and Scanning Electron Microscopic Study. *Journal of Microscopy and Ultrastructure*. (2020) 8: 69-74. doi: 10.4103/JMAU.JMAU_55_19.
2. Gao Y, Meng L, Liu H, Wang J and Zheng N: The Compromised Intestinal Barrier Induced by Mycotoxins. *Toxins Journal*. (2020) 12(10): 619-660. doi: 10.3390/toxins12100619.
3. Freeman HJ: Multifocal stenosing ulceration of the small intestine. *World Journal of Gastroenterology*. (2009) 15(39): 4883–4885. doi: 10.3748/wjg.15.4883.
4. Ebi M, Inoue S, Sugiyama T, Yamamoto K, Adachi K, Yoshimine T, *et al.*: A Small Bowel Ulcer due to Clopidogrel with Cytomegalovirus Enteritis Diagnosed by Capsule and Double-Balloon Endoscopy. *Case Reports in Gastroenterology*. (2018) 12(2): 303-310. doi: 10.1159/000490096.
5. Aly RM: Current state of stem cell-based therapies: an overview. *Stem Cell Investigation Journal*. (2020) 7: 8-17. doi: 10.21037/sci-2020-001.
6. Wang LL, Janes ME, Kumbhojkar N, Kapate N, Clegg JR, Prakash S, *et al.*: Cell therapies in the clinic. *Bioengineering & Translational Medicine Journal*. (2021) 26;6(2): e10214. doi: 10.1002/btm2.10214.
7. Aguiar FS, Melo AS, Araújo AMS, Cardoso AP, Souza SAL, Lopes-Pacheco M, *et al.*: Autologous bone marrow-derived mononuclear cell therapy in three patients with severe asthma. *Stem Cell Research & Therapy Journal*. (2020) 11: 167. doi: 10.1186/s13287-020-01675-x.

8. Suda S, Nito C, Yokobori S, Sakamoto Y, Nakajima M, Sowa K, *et al.*: Recent Advances in Cell-Based Therapies for Ischemic Stroke. *International Journal of Molecular Sciences*. (2020) 21: 6718-6741. doi: 10.3390/ijms21186718.
9. Sen P, Kemppainen E and Orešič M: Perspectives on Systems Modeling of Human Peripheral Blood Mononuclear Cells. *Frontiers in Molecular Biosciences*. (2018) 4: 96. doi: 10.3389/fmolb.2017.00096.
10. Wexler SA, Donaldson C, Denning-Kendall P, Rice C, Bradley B, and Hows JM: Adult bone marrow is a rich source of human mesenchymal 'stem' cells but umbilical cord and mobilized adult blood are not. *British Journal of Haematology*. (2003) 121: 368-374. doi: 10.1046/j.1365-2141.2003.04284.x.
11. Zhang M and Huang B: The multi-differentiation potential of peripheral blood mononuclear cells. *Stem Cell Research & Therapy Journal*. (2012) 3: 48-57. doi: 10.1186/scrt139.
12. Kang J, Kim T, Hur J and Kim H: Strategy to Prime the Host and Cells to Augment Therapeutic Efficacy of Progenitor Cells for Patients with Myocardial Infarction. *Frontiers in Cardiovascular Medicine*. (2016) 3 (46): 1-9. doi: 10.3389/fcvm.2016.00046.
13. Kang J, Hur J, Kang JA, Lee HS, Jung H, Choi J, *et al.*: Priming mobilized peripheral blood mononuclear cells with the "activated platelet supernatant" enhances the efficacy of cell therapy for myocardial infarction of rats. *Cardiovascular Therapeutics Journal*. (2016) 34: 245-253. doi: 10.1111/1755-5922.12194.
14. Hou Y and Li C: Stem/Progenitor Cells and Their Therapeutic Application in Cardiovascular Disease. *Frontiers in Cell and Developmental Biology Journal*. (2018) 6: 139-149. doi: 10.3389/fcell.2018.00139.
15. National Research Council of the National Academies: *Guide for the Care and Use of Laboratory Animals*. 8th edition. National Academies Press, Washington, D.C. (2011) pp: 41-104.
16. Turkyilmaz IB, Pirincci PA, Bolkent S and Yanardag R: The effects of vitamins and selenium mixture or ranitidine against small intestinal injury induced by indomethacin in adult rats. *Journal of Food Biochemistry*. (2019) 43(4): e12808. doi.org/10.1111/jfbc.12808.
17. Lyu H., Sun D.M., Chi Ping N.g., Cheng W.S., Chen J.F., He Y.Z., *et al.*: Umbilical Cord Blood Mononuclear Cell Treatment for Neonatal Rats with Hypoxic Ischemia. *Frontiers in Cellular Neuroscience*. (2022) 16: Article 823320. doi: 10.3389/fncel.2022.823320.
18. Gaertner DJ, Hallman TM, Hankenson FC and Batchelder MA: *Anesthesia and Analgesia in Rodents. Anesthesia and Analgesia in Laboratory Animals*. 2nd Edition, Academic Press, San Diego, CA. Boston. (2008) pp: 239-240. doi.org/10.1016/B978-0-12-373898-1.X5001-3.
19. Șerban GM, Mănescu IB, Manu DR and Dobreanu M: Optimization of a Density Gradient Centrifugation Protocol for Isolation of Peripheral Blood Mononuclear Cells. *Acta Medica Marisiensis*. (2018) 64 (2): 83-90. doi: 10.2478/amma-2018-0011.
20. Oellerich M and Dasgupta A: *Personalized Immunosuppression in Transplantation: Role of Biomarker Monitoring and Therapeutic Drug Monitoring*. 1st edition. Elsevier. Amsterdam. Oxford. London. Paris. Boston. Newyork. (2016) pp: 200-226. doi.org/10.1016/C2013-0-19247-1.
21. Escobar G, Escobar A, Ascuí G, Tempio FI, Ortiz MC, Pérez CA *et al.*: Pure platelet-rich plasma and supernatant of calcium-activated P-PRP induce different phenotypes of human macrophages. *Regenerative Medicine*. (2018) 13(4): 427-441. doi: 10.2217/rme-2017-0122.
22. Dhurat R and Sukesh MS: Principles and Methods of Preparation of Platelet-Rich Plasma: A Review and Author's Perspective. *Journal of Cutaneous and Aesthetic Surgery*. (2014) 7(4): 189-197. doi: 10.4103/0974-2077.150734.
23. Kim DH, Je YJ, Kim CD, Lee YH, Seo YJ, Lee JH *et al.*: Can platelet rich plasma be used for skin rejuvenation. Evaluation of effects of platelet rich plasma on human dermal fibroblast. *Annals of Dermatology Journal*. (2011) 23(4): 424-31. doi: 10.5021/ad.2011.23.4.424.
24. Quarteiro ML, Tognini JRF, Flores de Oliveira EL and Silveira I: The effect of platelet-rich plasma on the repair of muscle injuries in rats. *Revista Brasileira de Ortopedia Journal*. (2015) 50(5): 586-95. doi: 10.1016/j.rboe.2015.08.009.
25. Jo CH, Roh YH, Kim JE, Shin S and Yoon KS: Optimizing Platelet-Rich Plasma Gel Formation by Varying Time and Gravitational Forces During Centrifugation. *Journal of Oral Implantology*. (2013) 39(5): 525-32. doi: 10.1563/AAID-JOI-D-10-00155.
26. Cavallo C, Roffi A, Grigolo B, Mariani E, Pratelli L, Merli G, *et al.*: Platelet-Rich Plasma: The Choice of Activation Method Affects the Release of Bioactive Molecules. *BioMedical Research International Journal*. (2016) 2016: ID 6591717. doi: 10.1155/2016/6591717.
27. Suvarna SK, Layton C and Bancroft JD: *Bancroft's Theory and Practice of Histological Techniques*. 8th edition. Elsevier. Churchill Livingstone. (2019) pp: 73-83, 126-138, 215-238. doi.org/10.1016/C2015-0-00143-5.
28. Cheville NF and Stasko J: Techniques in electron microscopy of animal tissue. *Veterinary Pathology Journal*. (2014) 51(1): 28-41. doi: 10.1177/0300985813505114.

29. Ibrahim AA and Okasha EF: Effect of genetically modified corn on the jejunal mucosa of adult male albino rat. *Experimental and Toxicologic Pathology Journal*. (2016) 68: 579-588. doi: 10.1016/j.etp.2016.10.001.
30. Şensoy E and Öznurlu Y: Determination of the changes on the small intestine of pregnant mice by histological, enzyme histochemical, and immunohistochemical methods. *Turkish Journal of Gastroenterology*. (2019) 30(10): 917-24. doi: 10.5152/tjg.2019.18681.
31. Andrade C.: The P Value and Statistical Significance: Misunderstandings, Explanations, Challenges, and Alternatives. *Indian J Psychol Med*. (2019) 41: 210-215. doi: 10.4103/IJPSYM.IJPSYM_193_19.
32. Erben U, Loddenkemper C, Doerfel K, Spieckermann S, Haller D, Heimesaat MM, *et al.*: A guide to histomorphological evaluation of intestinal inflammation in mouse models. *International Journal of Clinical and Experimental Pathology*. (2014) 7(8):4557-4576. PMID: 25197329; PMCID: PMC4152019.
33. Ishii M, Fukuoka Y, Deguchi S, Otake H, Tanino T and Nagai N: Energy-Dependent Endocytosis Is Involved in the Absorption of Indomethacin Nanoparticles in the Small Intestine. *International Journal of Molecular Sciences*. (2019) 20 (3): 476-489. doi: 10.3390/ijms20030476.
34. Cervantes-García D, Bahena-Delgado AI, Jiménez M, Córdova-Dávalos LE, Palacios VR, Sánchez-Alemán E, *et al.*: Glycomacropeptide Ameliorates Indomethacin-Induced Enteropathy in Rats by Modifying Intestinal Inflammation and Oxidative Stress. *Molecules Journal*. (2020) 25: 2351-2368. doi: 10.3390/molecules25102351.
35. Bjarnason I and Takeuchi K: Intestinal permeability in the pathogenesis of NSAID-induced enteropathy. *Journal of Gastroenterology*. (2009) 44: 23-29. doi.org/10.1007/s00535-008-2266-6.
36. Kim EK, Cho JH, Jeong AR, Kim EJ, Park DK, Kwon KA, *et al.*: Anti-Inflammatory Effects of Simvastatin in Nonsteroidal Anti-Inflammatory Drugs-Induced Small Bowel Injury. *Journal of Physiology and Pharmacology*. (2017) 68(1): 69-77. PMID: 28456771.
37. Mahdavi FS, Mardi P, Mahdavi SS, Kamalinejad M, Hashemi SA, Khodaii Z, *et al.*: Therapeutic and Preventive Effects of *Olea europaea* Extract on Indomethacin-Induced Small Intestinal Injury Model in Rats. *Evidence-Based Complementary and Alternative Medicine journal*. (2020) 2020: ID 6669813. doi:10.1155/2020/6669813.
38. Sivalingam N, Basivireddy J, Balasubramanian KA and Jacob M: Curcumin attenuates indomethacin-induced oxidative stress and mitochondrial dysfunction. *Archives of Toxicology Journal*. (2008) 82: 471-481. doi: 10.1007/s00204-007-0263-9.
39. Boueiz A and Hassoun PM: Regulation of endothelial barrier function by reactive oxygen and nitrogen species. *Microvascular Research*. (2009) 77(1): 26-34. doi: 10.1016/j.mvr.2008.10.005.
40. Lai Y, Zhong W, Yu T, Xia Z, Li J, Ouyang H, *et al.*: Rebamipide Promotes the Regeneration of Aspirin-Induced Small-Intestine Mucosal Injury through Accumulation of β -Catenin. *PLoS ONE*. (2015) 10(7): e0132031. doi: 10.1371/journal.pone.0132031.
41. Korany DA, Said RS, Ayoub IM, Labib RM, El-Ahmady SH and Singab AB: Protective effects of *Brownea grandiceps* (Jacq.) against γ -radiation-induced enteritis in rats in relation to its secondary metabolome fingerprint. *Biomedicine & Pharmacotherapy Journal*. (2022) 146: 112603. doi.org/10.1016/j.biopha.2021.112603.
42. Yamamoto A, Itoh T, Nasu R and Nishida R: Sodium alginate ameliorates indomethacin-induced gastrointestinal mucosal injury via inhibiting translocation in rats. *World Journal of Gastroenterology*. (2014) 20(10): 2641-2652. doi: 10.3748/wjg.v20.i10.2641.
43. Xian CJ, Couper R, Howarth GS, Read LC and Kallincos NC: Increased expression of HGF and c-met in rat small intestine during recovery from methotrexate-induced mucositis. *British Journal of Cancer*. (2000) 82(4): 945-952. doi.org/10.1054/bjoc.1999.1023.
44. Nagano Y, Matsui H, Muramatsu M, Shimokawa O, Shibahara T, Yanaka A, *et al.*: Rebamipide Significantly Inhibits Indomethacin-Induced Mitochondrial Damage, Lipid Peroxidation, and Apoptosis in Gastric Epithelial RGM-1 Cells. *Digestive Diseases and Sciences*. (2005) 50: S76-S83. doi: 10.1007/s10620-005-2810-7.
45. Abdelmeguid NE, Fakhoury R, kamal SM and Al Wafai RJ: Effects of *Nigella sativa* and thymoquinone on biochemical and subcellular changes in pancreatic β -cells of streptozotocin-induced diabetic rats. *Journal of Diabetes*. (2010) 2: 256-266. doi: 10.1111/j.1753-0407.2010.00091.x.
46. Kumar V, Abbas AK and Aster JC: *Robbins and Cotran Pathologic Basis of Disease*. 10th edition. Elsevier INC, China. (2021) pp: 1-56.
47. Stevens A and Lowe J: *Pathology*, 2nd edition, Mosby, London, New York, (2000) pp: 26.
48. Ali SS, ElGibaly RI and Abdel-Maksoud SA: Effect of *Musa sapientum* (Banana) on Indomethacin-Induced Gastric Mucosal Injury in Rats: Histological Study. *Journal of Medical Histology*. (2018) 2(1): 11-28. doi:10.21608/jmh.2018.4452.1034.

49. Abdel Mohsen AF, Salama NM, Rashed LA, Farag EA and Abdel Hameed AM: A Comparative Histological Study on the Effect of Adipose-Derived Stem Cells versus Their Conditioned Medium on Indomethacin Induced Enteritis in Adult Female Albino Rats. *The Egyptian Journal of Histology*. (2018) 41(4): 503-519. doi:10.21608/ejh.2018.4351.1014.
50. El Ghazzawy IF, Meleis AE, Farghaly EF and Solaiman A: Histological study of the possible protective effect of pomegranate juice on bisphenol-A induced changes of the caput epididymal epithelium and sperms of adult albino rats. *Alexandria Journal of Medicine*. (2011) 47: 125-137. doi.org/10.1016/j.ajme.2011.06.006.
51. Maclachlan NJ and Dubovi EJ: *Fenner's Veterinary Virology*. 4th edition. Academic Press. (2011) pp: 43-74. doi.org/10.1016/C2009-0-01816-9.
52. Chamoun-Emanuelli AM, Bryan LK, Cohen ND, Tetrault TL, Szule JA, Barhoumi R, *et al.*: NSAIDs disrupt intestinal homeostasis by suppressing macroautophagy in intestinal epithelial cells. *Scientific Reports*. (2019) 9:14534-14548. doi.org/10.1038/s41598-019-51067-2.
53. Dehler M, Zessin E, Bartsch P and Mair-Baur H: "Hypoxia causes permeability oedema in the constant-pressure perfused rat lung". *European Respiratory Journal*. (2006) 27(3): 600-606. doi: 10.1183/09031936.06.00061505.
54. Lundgren J and Radegran G: "Pathophysiology and potential treatments of pulmonary hypertension due to systolic left heart failure". *Acta Physiologica (Oxf)*. (2014) 211(2): 314-333. doi: 10.1111/apha.12295.
55. Ahmed OF, Shalaby SA, Ibraheem EM, Metwally AG and Manawy SM: A Comparative Study between the Therapeutic Role of Bone Marrow Mesenchymal Stem Cells and that of Histamine2 Receptor Antagonists (Nizatidine) in the Management of Ibuprofen Induced Gastric Ulcer in Adult Albino Rats. *Benha Medical Journal*. (2020) 37(3): 678-690. doi: 10.21608/BMFJ.2020.112176.
56. Ornellas FM, Ornellas DS, Martini SV, Castiglione RC, Ventura GM, Rocco PR, *et al.*: Bone Marrow-Derived Mononuclear Cell Therapy Accelerates Renal Ischemia-Reperfusion Injury Recovery by Modulating Inflammatory, Antioxidant and Apoptotic Related Molecules. *Cellular Physiology and Biochemistry Journal*. (2017) 41: 1736-1752. doi: 10.1159/000471866.
57. Ramli Y, Alwahdy AS, Kurniawan M, Juliandi B, Wuyung PE and Susanto YDP: Intravenous Versus Intraarterial Transplantation of Human Umbilical Cord Blood Mononuclear Cells for Brain Ischemia in Rats. *HAYATI Journal of Biosciences*. (2017) 24(4): 187-194. doi.org/10.1016/j.hjb.2017.11.002.
58. Zaghlool SS, Abo-Seif AA, Rabeh MA, Abdelmohsen UR and Messiha BAS: Gastro-Protective and Antioxidant Potential of *Althaea officinalis* and *Solanum nigrum* on Pyloric Ligation/Indomethacin-Induced Ulceration in Rats. *Antioxidants*. (2019) 8: 512-542. doi: 10.3390/antiox8110512.

الملخص العربي

التأثير العلاجي لخلايا الدم الطرفية وحيدة النواة المستنفرة المدعمة بطاف الصفائح الدموية المنشطة على القرحة المستحثة تجريبياً في اللفانفي لذكر الجرذ الأبيض البالغ: دراسة هستولوجية وهستوكيميائية مناعية

آية عبد المنعم أبو اليزيد^١، أميرة عدلى كساب^{١،٢}، نادية عبد المحسن البكري^١، عزه عوض أبوريه^١،
نوار محمود شلبي^١

^١ قسم الهستولوجيا وبيولوجيا الخلية- كلية الطب- جامعة طنطا

^٢ قسم العلوم الطبية الأساسية، كلية الطب، جامعة ابن سينا للعلوم الطبية، عمان، الأردن

المقدمة: عادة ما تحدث قرحة الأمعاء الدقيقة لعدد من الأسباب و تمثل الأدوية غير الستيرويدية المضادة للإلتهابات الأسباب الأكثر شيوعاً للإصابة المستحثة بالأدوية للأمعاء الدقيقة. يلعب العلاج بخلايا الدم الطرفية وحيدة النواة دوراً هاماً في التئام الأنسجة وإصلاحها ، ومن المعروف أن تدعيمها بطاف تنشيط الصفائح الدموية يزيد من فعاليتها من خلال تحفيز تولد الأوعية الدموية وتجديد الأنسجة.

الهدف من العمل: تم إجراء هذا العمل لدراسة تأثير خلايا الدم الطرفية وحيدة النواة المدعمة بطاف الصفائح الدموية المنشطة على القرحة المستحثة بالاندوميثاسين في اللفانفي في ذكر الجرذ الأبيض البالغ.

المواد والطرق: تم استخدام ٤٥ من ذكور الجرذان البيضاء البالغة ، أستخدم ١٠ منهم كمتبرعين و ٣٥ الآخرين كمتلقين. حيث قسمت الجرذان المتلقية إلى ؛ المجموعة الأولى لتمثل المجموعة الضابطة ، المجموعة الثانية والتي تم تقسيمها إلى المجموعة الفرعية II-A (تم إعطاء الحيوانات جرعة واحدة عن طريق الفم من الإندوميثاسين ٢٥مجم/كجم وتم ذبح الحيوانات بعد ٦ ساعات من إحداث القرحة) ، والمجموعة الفرعية II-B (عولجت بخلايا الدم الطرفية وحيدة النواة المزودة بطاف الصفائح الدموية المنشطة عن طريق الحقن في الوريد بعد احداث القرحة وتم ذبح الحيوانات بعد أسبوعين). في النهاية، تم أخذ اللفانفي ومعالجته للفحص الهستولوجي والهستوكيميائي المناعي.

النتائج: لقد أظهرت المجموعة الفرعية II-A تغيرات تركيبية ملحوظة مثل تلف في بعض المناطق، ضمور في الزغابات (الخمالات)، انفضال الخلايا، أنوية داكنة، وفجوات في السيتوبلازم. وقد أحدث العلاج بخلايا الدم الطرفية وحيدة النواة المدعمة بطاف الصفائح الدموية المنشطة تحسناً ملحوظاً في التركيب الهستولوجي للنفانفي (المجموعة الفرعية II-B).

الخاتمة: خلايا الدم الطرفية وحيدة النواة المدعمة بطاف الصفائح الدموية المنشطة لها تأثيراً محسناً جيداً على اللفانفي بعد إحداث القرحة.